00-100

Environment Canada
Water Science and Technology Directorate

Direction générale des sciences et de la technologie, eau
Environnement Canada

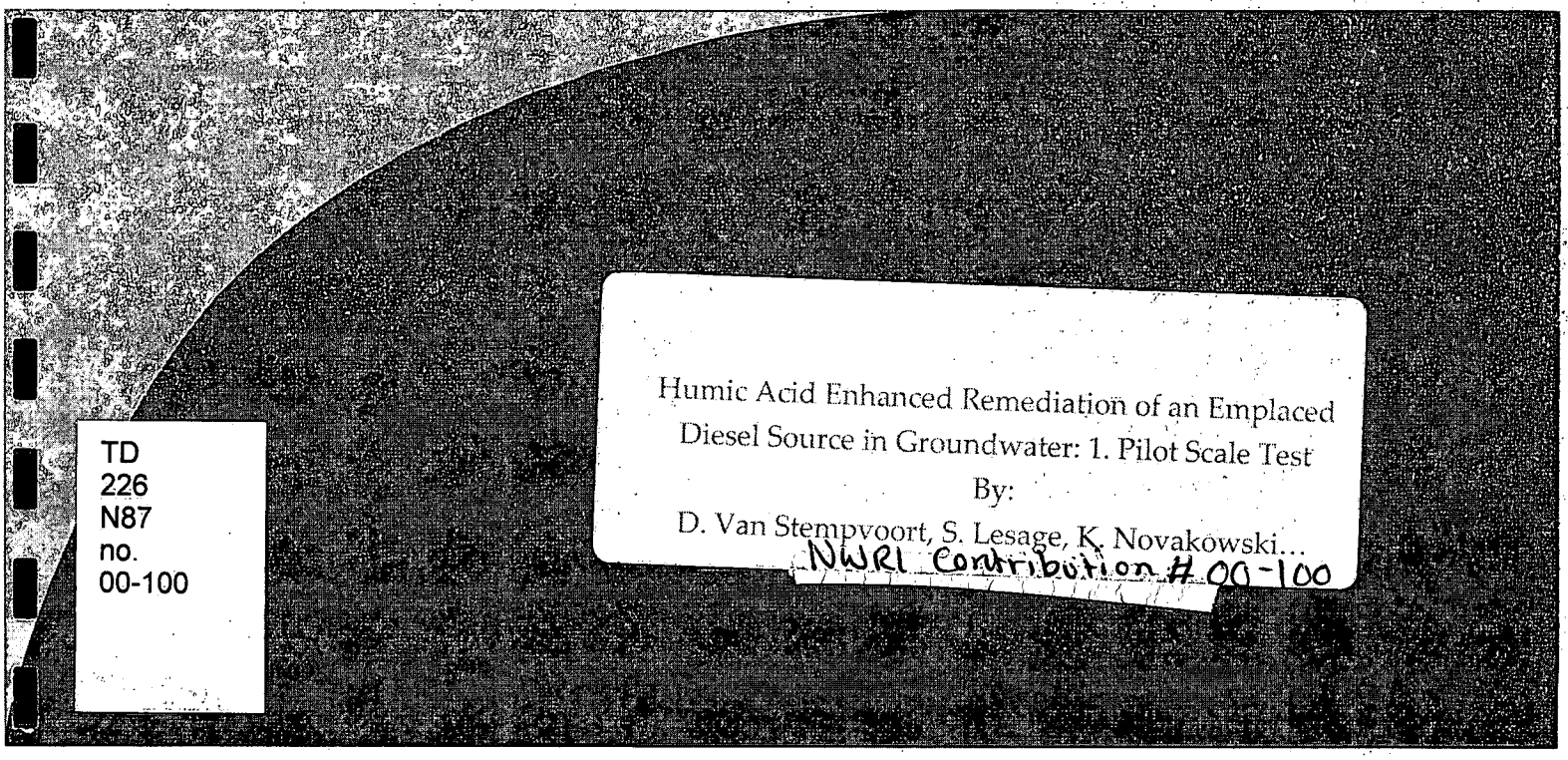

Humic Acid Enhanced Remediation of an Emplaced Diesel Source in Groundwater: 1. Pilot Scale Test

By:

D. Van Stempvoort, S. Lesage, K. Novakowski...

00-100

D. R. Van Stempvoort, D.R., Lesage, S., Novakowski, E. K., Millar, K. and Brown, S. Humic Acid Enhanced Remediation of an Emplaced Diesel Source in Groundwater: 1. Pilot Scale Test.

Management Perspective

This manuscript, prepared for publication in Journal of Contaminant Hydrology, describes research that was funded by the Panel for Energy Research and Development (PERD). Information is provided on the testing and development of a novel groundwater remediation technology, which is of interest to the groundwater remediation service industry in Canada, and contributes toward Environment Canada's Clean Environment theme. The intended result is that the environmental and human health threats posed by toxic substances and other substances of concern are prevented or reduced.

The manuscript describes a test of enhanced flushing of PAH contaminants from a diesel fuel source in groundwater, using a commercial humic product as a flushing agent. This test was conducted in a model sand aquifer at the pilot scale in the AQUEREF facility at the Canada Centre for Inland Waters, Burlington, Ontario. Monitoring data showed that the bulk of the methylated naphthalenes (PAHs) that were liberated from the diesel were biodegraded within the model aquifer. The use of this technology may increase the efficiency of active groundwater remediation. A joint paper (Part 2) in collaboration with the University of Waterloo provides numerical modeling of the experimental data.

Assainissement amélioré par l'acide humique d'une source ponctuelle de carburant diesel contaminant l'eau souterraine : 1. Essais à l'échelle pilote.

Van Stempvoort, D. R., Lesage, S., Novakowski, E. K., Millar, K. et Brown, S.

Sommaire à l'intention de la direction

Ce manuscrit, rédigé pour le Journal of Contaminant Hydrology, décrit des recherches financées par le Groupe interministériel de recherche et d'exploitation énergétiques (GRDE). On présente des informations sur les essais et le développement d'une nouvelle technologie d'assainissement des eaux souterraines, utiles pour l'industrie des services d'assainissement des eaux souterraines du Canada, et qui s'insère dans le secteur d'activité Un environnement sain d'Environnement Canada. Les résultats attendus sont la prévention ou la réduction des dangers pour l'environnement et la santé humaine posés par les substances toxiques et d'autres substances préoccupantes.

Ce manuscrit décrit l'essai d'une technique améliorée de purge des contaminants HAP d'une source de carburant diesel se diffusant dans l'eau souterraine, qui utilise un produit humique du commerce comme agent de purge. On a effectué cet essai à l'échelle pilote dans un aquifère de sable artificiel à l'installation AQUEREF du Centre canadien des eaux intérieures de Burlington (Ontario). Les données de surveillance ont montré que la plus grande partie des naphtalènes méthylés (HAP) qui étaient libérés par le carburant diesel étaient biodégradés dans l'aquifère artificiel. L'utilisation de cette technologie peut augmenter l'efficacité des techniques actives d'assainissement des eaux souterraines. Un document connexe (partie 2), rédigé en collaboration avec l'Université de Waterloo, décrit la modélisation numérique des données expérimentales.

Abstract

The enhanced solubility of petroleum-derived compounds in humic acid solutions is the basis for the development of a new groundwater remediation technology. In this unique pilot-scale test, a stationary contaminant source consisting of diesel fuel was placed below the water table in a model sand aquifer (1.2 m x 5.5 m x 1.8 m deep) and flushed with water at a flow rate of 2 cm/h over 5 years. At 51 d, laboratory grade humic acid was added to the water and maintained at a level of 0.8 to 1.0 g/L. The addition of humic acid had only a small impact on the mobilization of the BTEX components, which were rapidly flushed from the diesel, but had a large effect on the flushing of PAHs, including methylated naphthalenes (MNs). Binding to aqueous humic acid enhanced the solubilization of MNs two to ten fold. During transport, biodegradation of the BTEX and PAHs occurred, limiting the lateral and longitudinal extent of the diesel contaminant plume in the model aquifer. It appears that through enhanced solubilization, the biodegradation rate of the MNs was increased. As the various MNs were depleted from the diesel source, the MN plume shrank and then disappeared.

Résumé

Pour le développement d'une nouvelle technologie d'assainissement des eaux souterraines, on s'est basé sur la plus grande solubilité des composés du pétrole dans une solution d'acide humique. Lors de cet essai innovateur à l'échelle pilote, on a placé une source de contaminant fixe constituée de carburant diesel sous la surface de la nappe d'un aquifère de sable artificiel (1,2 m x 5,5 m x 1,8 m de profondeur), lessivé par un écoulement d'eau à un débit de 2 cm/h pendant 5 ans. Au 51^{e} jour, on a ajouté de l'acide humique de qualité laboratoire à l'eau et on a maintenu sa concentration à 0,8 -1,0 g/L. L'addition d'acide humique n'avait qu'un faible impact sur la mobilisation des composés du BTEX, qui étaient rapidement purgés du carburant diesel, mais elle avait un effet important sur la purge des HAP, notamment des naphtalènes méthylés (NM), car leur liaison aux acides humiques aqueux améliorait leur solubilisation par un facteur de 2 à 10. Pendant le transport, on notait une certaine biodégradation des BTEX et des HAP, ce qui limitait l'étendue latérale et longitudinale du panache des contaminants du carburant diesel dans l'aquifère artificiel. Il semble donc que cette amélioration de la solubilisation augmentait la vitesse de biodégradation des NM. Avec l'épuisement progressif des divers NM dans le source de carburant diesel, le panache de NM s'est rétréci et a finalement disparu.

ELSEVIER

Journal of Contaminant Hydrology 54 (2002) 249–276

JOURNAL OF
Contaminant
Hydrology

www.elsevier.com/locate/jconhyd

Humic acid enhanced remediation of an emplaced diesel source in groundwater. 1. Laboratory-based pilot scale test

D.R. Van Stempvoort [a,*], S. Lesage [a], K.S. Novakowski [a,1], K. Millar [a], S. Brown [a], J.R. Lawrence [b]

[a] *National Water Research Institute, P.O. Box 5050, Burlington, ON, Canada L7R 4A6*
[b] *National Water Research Institute, 11 Innovation Boulevard, Saskatoon, Saskatchewan, Canada S7N 3H5*

Received 8 January 2001; received in revised form 20 July 2001; accepted 5 September 2001

Abstract

The enhanced solubility of petroleum-derived compounds in humic acid solutions is the basis for a new groundwater remediation technology. In this unique pilot-scale test, a stationary contaminant source consisting of diesel fuel was placed below the water table in a model sand aquifer (1.2 × 5.5 × 1.8-m deep) and flushed with water at a flow rate of 2 cm/h over 5 years. At 51 days, laboratory grade humic acid was added to the water and maintained at a level of approximately 0.8 g/l. The addition of humic acid had only a small impact on the aqueous transport of the BTEX components, which were rapidly dissolved from the diesel, but had a large effect on the flushing of PAHs, including methylated naphthalenes (MNs). Binding to aqueous humic acid enhanced the solubilization of MNs two- to tenfold. During aqueous transport, biodegradation of the BTEX and PAHs occurred, limiting the lateral and longitudinal extent of the diesel contaminant plume in the model aquifer. It appears that through enhanced solubilization, the overall biodegradation rate of the MNs was increased. As the various MNs were depleted from the diesel source, the MN plume shrank and then disappeared.

Keywords: Diesel; Naphthalene; BTEX; Humic acid; Solubilization; Remediation

* Corresponding author. Tel.: +1-905-319-6917; fax: +1-905-336-6430.
E-mail address: dale.vanstempvoort@ec.gc.ca (D.R. Van Stempvoort).
[1] Current address: Department of Civil Engineering, Queen's University, Kingston, ON, Canada K7L 3N6.

0169-7722/02/$ - see front matter
PII: S0169-7722(01)00182-6

1. Introduction

The use of light petroleum products (e.g., gasoline, diesel fuel) is common throughout the world, and contamination of groundwater by such products is widespread. More restrictive regulations and better designs for underground storage tanks should reduce such problems in the future, but numerous existing contaminated sites must be cleaned up. Petroleum contamination can occur in the soil, the vadose zone, and the groundwater (i.e., below the water table). At some sites, the contaminated soils and vadose zones are excavated and treated in biopiles, or remediated by in-situ techniques such as bioventing. In order to remediate the groundwater, active technologies such as pump-and-treat or in-situ bioremediation (e.g., biosparging) are often used, although a new approach, monitored natural attenuation, is growing in importance (Chapelle, 1999). The efficiencies of active techniques, such as pump-and-treat or in-situ bioremediation, are limited by the presence of nonaqueous phase liquid (NAPL) petroleum, which sometimes is present below the water table. This occurs when a fraction of the NAPL that forms a layer or pool above the water-saturated zone becomes trapped as droplets within the sediment pores as the water table rises.

Generally, the main factor limiting active remediation techniques is the low aqueous solubility of petroleum hydrocarbon(s) or other organic contaminants (Brubaker, 1991). The addition of an organic carrier to the groundwater may significantly enhance the solubilization and mobility of the contaminants, and hence improve the efficiency of active remediation. This approach, referred to as in-situ flushing, is a relatively new technology (Roote, 1998). Various chemical flushing agents have been tested, including surfactants (West and Harwell, 1992; Sabatini et al., 2000), biosurfactants and other biosynthesized compounds (e.g., Barkay et al., 1999; Noordman et al., 2000), polymers (Martel et al., 1998), miscible cosolvents such as alcohols (Rao et al., 1997; Falta, 1998), surfactant/cosolvent mixtures (Martel and Gélinas, 1996; Bettahar et al., 1999) and commercial humic products (Abdul et al., 1990; Xu et al., 1994; Lesage et al., 1995; Johnson and John, 1999; Boving and Brusseau, 2000; this study). There are very few published studies that provide direct comparisons of the use of alternative carriers (e.g., Boving and Brusseau, 2000). Subject to further research and development, we suggest that for some applications, the use of commercial humic products may offer several advantages over other carriers, such as lower cost, lower toxicity, and greater persistence (e.g., surfactants may be readily biodegraded, some are toxic).

In this paper we describe the first pilot-scale test of the use of a commercial humic product as a carrier in groundwater remediation. In this test, we added Aldrich humic acid (1 g/l) to enhance the remediation of diesel fuel in a model aquifer. Bench-scale batch and column tests that were conducted in support of this pilot-scale test are reported elsewhere (Xu et al., 1994; Van Stempvoort et al., 2000; Van Stempvoort and Lesage, in press). The pilot-scale test reported here represents an important step in the research and development phase of this proposed remediation technology, following promising results at the bench scale. Field tests are often marred by problems related to the heterogeneous properties of aquifers (e.g., Mas-Pla et al., 1992). Thus, we decided to study the movement of both the humic acid carrier and contaminants at the pilot scale in a laboratory setting. This paper provides a detailed description of the methods and the results of the pilot scale experiment.

This paper also serves as an introduction for a companion paper that develops a 3D numerical model of the experiment, including the transport of humic acid and diesel contaminants, and concurrent biodegradation (Molson et al., this issue).

2. Materials and methods

2.1. Construction of pilot scale aquifer flow cells

In the AQUEREF laboratory facility at the Canada Centre for Inland Waters, Burlington, Ontario, a pilot-scale, rectangular (2.4 × 6.1 × 1.8-m deep) reservoir was constructed. This reservoir was made of 1/4-in. industrial grade stainless steel, with external steel beams for support. At one end of this reservoir, a head tank (2.4 × 0.6 × 1.8-m deep) was formed by installing a perforated vertical wall (1/4-in. stainless steel with 1-in. diameter, quincuncial holes). The porosity of this wall was >0.3. The remaining volume of the reservoir was divided into two equal-sized flow cells (1.2 × 5.5 × 1.8-m deep) (Fig. 1) by installing a second vertical wall consisting of a 0.025-in. thick stainless steel sheet (T304, Atlas Alloys, Etobicoke, ON). The gap between the lower edge of this sheet and the reservoir floor was sealed with bentonite to prevent cross-flow. In the two flow cells, monitoring wells were suspended from a wooden frame at intervals of 25 to 30 cm. The resulting monitoring array in each flow cell was four rows (A to D), each containing 8 to 10 monitoring bundles, with wells at five depths in each bundle (Figs. 1 and 2). The wells were made of stainless steel tubes (3-mm i.d., nominal 1/8-in. o.d.) terminated with stainless steel porous cups (Gasmac, Guelph, ON: 40-μm pores, 0.25-in.

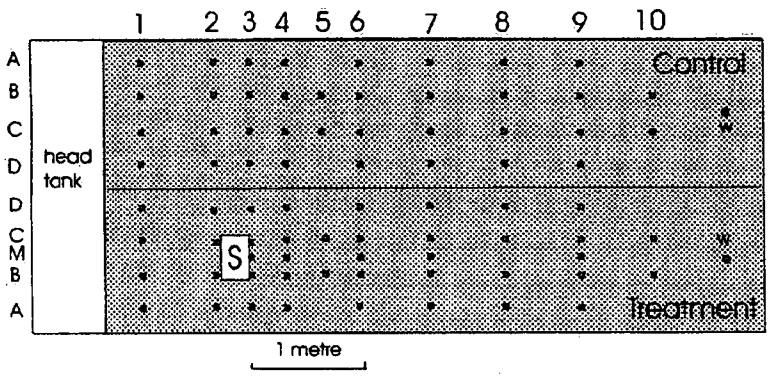

Fig. 1. Plan view of flow cells. Locations of monitoring bundles (5 wells per bundle) are shown as small solid rectangles, withdrawal wells as solid circles (W). The 4- or 5-digit location code for each monitoring point (e.g., T3B4), is as follows: (i) first digit, T or C for treatment or control cell; (ii) second–third digit(s), number between 1 to 10 referring to column in bundle array; (iii) third/fourth digit, letter between A and D, row in bundle array; (iv) number between 1 and 5, level of well intake zone (depth; see Fig. 2). The large rectangle labelled "S" is the diesel source.

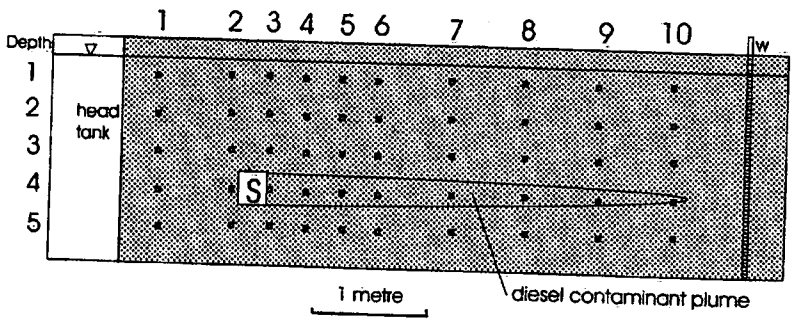

Fig. 2. Profile of the treatment flow cell (cross section through row A), showing monitoring points (solid rectangles) at five depths, the diesel source (large rectangle labelled "S"), and the extraction well ("W"). See Fig. 1 for plan view of this system.

o.d., 0.125-in. i.d., 1-in. long). Injection wells (temporary) and withdrawal wells were installed at the head and toe ends of each flow cell, respectively (Figs. 1 and 2). Each of these four wells was constructed with PVC tubing (5-cm o.d.) screened over the entire length (2 m). To provide a porous model aquifer material, 40 t of medium to very coarse (Table 1) carbonate-rich "Winter Sand" was obtained from a local aggregate supplier (Preston Sand and Gravel, Kitchener, ON, Canada). A layer of polyester geotextile (250 μm: B and SH Thompson, Scarborough, ON) was placed over the perforated plates in the flow cells, and then both cells were filled with Winter Sand. The sides of the flow cells were then tapped with a mallet to assist the consolidation of the sand. A layer of plastic film was placed over the sand, and the pore space within this sediment was purged with He for 4 days, to remove O_2 and limit aerobic degradation during subsequent testing. He was introduced through the two injection wells and removed by a pair of peristaltic pumps (Cole-Parmer no. 7553-70) at the two withdrawal wells. Packers were placed in the injection and withdrawal wells to prevent inadvertent mixing of He with ambient air. Tap water (municipal supply derived from Lake Ontario) was then added by gravity to this system over the period of 1 week to saturate the sand, to a level ~ 0.2 m below the top of the head tank.

Table 1
Particle size distribution of Winter Sand, as reported by the supplier

Particle size (mm) by sieve	Weight percent (wt.%)
>4.75	0
2.36–4.75	25.3
1.18–2.36	34.7
0.60–1.18	30.0
0.30–0.60	9.0
0.15–0.30	0.5
0.075–0.15	0.2
<0.075	0.3

During subsequent testing, water was removed at a steady rate of 200 ml/min from each of the two withdrawal wells by the two peristaltic pumps. Fresh tap water (and later humic acid solution, see below) was introduced by gravity from one of two 833-l polyethylene reservoirs through a float valve placed in the head tank, at the same rate as total withdrawal (400 ml/min). The resulting steady level of water in the head tank initiated an even flow field through the perforated plate into the flow cells. In this way, steady flow conditions in the two cells were closely duplicated. All experiments were conducted at room temperature, generally 23 ± 2 °C. However, in spite of the heating of this space, the room temperature fluctuated seasonally between 15 and 27 °C. These fluctuations may have had some effect on biodegradation rates within the model aquifer, although we suspect that O_2 limitation was more important (see Section 4.2).

2.2. Tracer experiment

A tracer experiment was conducted to determine the hydraulic properties of the saturated-sand (model aquifer) flow cells using two chemical tracers: fluorescent lissamine (2 mg/l), and sodium bromide (100 mg/l). This test has been described elsewhere (Lesage et al., 2001). Preliminary 1D modeling of the bromide data indicated a longitudinal dispersivity of 0.005–0.015 m, a porosity of 28–32% and an average linear velocity of 0.020–0.022 m/h. These parameters were assumed to be applicable for the subsequent diesel flushing experiment.

2.3. Placement of a diesel source and establishment of a contaminant plume

The results of the tracer experiment were used to optimize the placement of a contaminant source in one of the flow cells, which was designated as the treatment cell. The second flow cell was retained as a control. Prior to source emplacement, an additional row (M) of five bundles (25 wells) was added to the monitoring network in the treatment cell, centred between rows B and C (Fig. 1).

To place the source, the water table was lowered to a depth of 1.6 m below the top of the cells. Then a rectangular excavation was made to 1.3 m, centred between bundles 2 and 3 in rows B and C (Fig. 1), by lowering a wooden frame (20 cm × 40 cm × 2 m i.d.) vertically into the treatment cell and removing the Winter Sand within the frame with a ShopVac™. This sand was temporarily placed on a clean tarp. In a preliminary column experiment, it was determined that the maximum concentration of diesel that could be trapped by capillary forces in the pores of the Winter Sand was 25 ml/kg. A 25-kg portion of the Winter Sand was dewatered and placed in a heavy clear plastic bag, then 500 ml of diesel (ESSO Petroleum, local supplier) was mixed with it, using a rolling and kneading action. This "diesel source" was placed at the bottom of the excavation in the treatment cell. This source was rectangular in shape (20 cm parallel to water flow × 40 cm perpendicular × 25-cm high), centred at monitoring depth 4 (Fig. 2). The excavation was then back-filled with the Winter Sand that had been removed, while the wooden form was slowly removed using an overhead pulley. The water table and steady flow in the cells were reestablished by adding fresh tap water to the head tank and pumping at the withdrawal wells. N_2 was bubbled into the head tank using diffusers, to remove dissolved

O_2. An activated carbon drum was used to remove hydrocarbons from the treatment flow cell effluent, prior to discharging this water to a floor drain.

2.4. Addition of humic acid

Humic acid was obtained as the sodium salt (tech., product no. H16752, Lot no. 16206AN, Aldrich Chemicals, Milwaukee, WI). We chose this product because most investigators of the binding of organic contaminants by commercial humic products have studied Aldrich humic acid (e.g., see recent compilations by Burkhard, 2000; Krop et al., 2001). At day 51 after the emplacement of the diesel source, a concentrated solution of this humic acid was poured into the head tank and the mixture stirred to produce a nominal concentration of 1 g/l humic acid. As a result of the humic acid addition, the pH of the water in the head tank increased from 6.5 to 7.9. To maintain a steady concentration of humic acid in the head tank, a new influent reservoir solution had been prepared in advance (833-l batch of 1 g/l Aldrich humic acid in tap water, polyethylene tank), and this batch was gravity-fed into the head tank, instead of tap water. Subsequently, two reservoirs of 1 g/l humic acid were used. As necessary, a new batch was prepared in one reservoir, while the other batch discharged to the head tank.

Downgradient of the withdrawal wells, the effluent from the carbon drum filter, was discarded (floor drain), until its humic acid concentration approached a constant level. From this time forward, the humic acid-rich water was recycled to the influent reservoir, with incremental addition of humic acid through a metering pump to make up for the losses by sorption to the aquifer and carbon drum filter.

Over a period of 145 days after the initial addition of the humic acid to the head tank (i.e., 196 days after source emplacement), water samples were collected from the monitoring network and analyzed for humic acid concentration by UV/Vis spectrophotometry (Varian Model CARY3) at 400 nm.

2.5. Monitoring of diesel plume

Following the diesel source emplacement, air samples were collected periodically from the upper few centimeters of the vadose zone (immediately below the plastic film) by glass syringe, to determine whether there were any vertical losses of volatile hydrocarbons during the re-saturation of the flow cells. During this time, water samples were also collected from all four monitoring levels in row M, using dedicated syringes (plastic, 30 ml). Each sample was immediately transferred to a 20-ml glass vial, which was filled and sealed with a Teflon-lined cap, following which, 5 ml was withdrawn by syringe to create a headspace. Analyses of volatile aromatics (BTEX) in the air samples and headspaces of the water samples were conducted within 1 h of collection by a Photovac 10S Plus gas chromatograph and detector system (flow of ultrazero air at 8 ml/min; oven at 50 °C; CPSIL 5CB column, PID).

Over 100 days following the emplacement of the diesel source, water was periodically sampled from the monitoring network and analyzed for concentrations of volatile aromatics (BTEX). The samples were transferred immediately to 40-ml glass vials, and analyzed by the Photovac system, as above. Peak confirmation was performed by GC/MS

(Hewlett Packard, Model 5890A GC, 5970 MSD). Also, a sample of the diesel was dissolved in methanol, diluted in water and placed in the purge cell for volatile organic analyses by GC/MSD. This provided the initial concentrations of BTEX in the diesel.

Previous studies have shown that methylated naphthalenes (MNs) are some of the most abundant PAHs in water contaminated by diesel (Thomas and Delfino, 1991; Lee et al., 1992; Xu et al., 1994). In this study, the initial abundances of MNs in the test diesel source were determined by HPLC. Samples of the diesel were diluted in methanol, then injected by autosampler into a 600E Waters HPLC system (Milford, USA), through a C8 Spheri-10 Brownlee™ column (4.6 mm × 3 cm) and a Waters 470 fluorescence detector. An isocratic system was used (50% acetonitrile in water). This set-up allowed mono-, di- and trimethylnaphthalenes to be distinguished without separation of individual isomers. Consequently, each peak, which contains a mixture of isomers, is considered a single compound: methylnaphthalene (MN), dimethylnaphthalene (DMN) and trimethylnaphthalene (TMN), respectively. The following isomers were used as standards: 1-MN; 1,3-DMN or 2,3-DMN; 2,3,5-TMN or 2,3,6-TMN (Aldrich Chemicals).

For analyses of aqueous MNs in the diesel contaminant plume, water samples were collected periodically over a 5-year period from the monitoring network. The water samples were collected by dedicated syringes, immediately transferred to 20-ml glass vials, and later to 5-ml autosampler vials. Samples were injected by autosampler into the 600E Waters HPLC system, using the same column, eluent and detector as above, for the diesel analysis. For a few of the water analyses, 1,3-DMN was substituted for 2,3-DMN, and 2,3,5-TMN for 2,3,6-TMN, as the reference standards. The nominal aqueous concentrations of MNs detected by HPLC include both dissolved and humic acid-bound fractions (Van Stempvoort and Lesage, in press).

Within several weeks of source emplacement, the trends in the distribution of the concentrations of MNs in the model aquifer indicated that biodegradation was playing an important role in the in-situ remediation of diesel contaminants. To assist the biodegradation process, air was bubbled into the head tank in place of N_2 at 248 days after source emplacement, and for the following 6 months, followed by O_2 for the duration of the test. To supplement the analyses of MNs, and to gain further insight into the biodegradation of these PAHs, the concentrations of dissolved oxygen were measured periodically at various monitoring points using an Orion 830 meter with a galvanic D.O. probe (#83010). The monitoring indicated losses of hydrocarbons and O_2 within the plume downgradient of the diesel source (Sections 3.2 and 3.3). Eventually, it was established that the breakthrough of dissolved MNs at the withdrawal well had ceased due to biodegradation (see Section 3.3). Accordingly, 180 days after the source emplacement, the carbon filter was removed from the water recycling circuit.

A change in eluent was made for the final two suites of HPLC analyses. At this time, it was observed that the humic acid in the water samples aggregated and precipitated out readily in the presence of acetonitrile. This was apparently due to aging of the humic acid; fresh aqueous humic acid did not precipitate in the presence of acetonitrile. The HPLC eluent was changed to 65% methanol in water, and the samples were pre-diluted (1:1) in methanol. For the last sampling event, the addition of methanol also induced precipitation of humic acid in the samples. Thus, for this event, the sample–methanol mixtures were centrifuged to remove the precipitate from the water column. Testing at that time showed

that the presence of humic acid precipitate in these 50% methanol mixtures had little effect on the HPLC analyses of the concentrations of total aqueous MNs.

2.6. Microbial analyses

Water samples were collected at 400 days, and bacterial counts were conducted by the spread plate method on plate count agar (American Public Health Association, 1995). To determine the lateral distribution of bacteria in the system, samples were collected from the head tank, the withdrawal wells, at level 4 from all monitoring wells in the treatment cell, and from selected rows (3, 6, and 9) at depth 4 in the control cell. A vertical distribution of bacteria in the treatment cell was determined using samples collected from the central monitoring wells of rows 3, 4, 6, 7 and 9, at all depths. Samples were diluted 100 × in sterile phosphate buffer, which was prepared using APHA Standard Method 9050C (American Public Health Association, 1995); 250-μl aliquots were spread on the prepared medium and incubated for 3 days, at room temperature, prior to enumeration.

At the completion of the test, samples of the Winter Sand were collected from the diesel source, and centrally (level 4 between rows 4 and 5) in both the treatment and control cells, using a Geoprobe® soil sampler (Salina, KS). Some samples were sent the same day, on ice, to Microbial Insights, Rockford, TN, for 16S rDNA and phospholipid fatty acid extraction and characterization. Other diesel source samples were stored at 5 °C, then stained with Syto9 (Molecular Probes, Eugene, OR) (green), and the lectins (Sigma, St. Louis, MI) *Triticum vulgaris* TRITC (red) and *Tetragonolobus purpureas* CY5 (blue). CY5 labelling was carried out using the commercial system supplied by Rockwell Chemicals. See Neu et al. (2001) regarding details of the application of fluor conjugated lectins to environmental samples. These preparations were examined using a Bio-Rad MRC 1024 confocal laser scanning system, on a Nikon Microphot SA microscope with 0.75 NA 20X air objective lens. The resulting confocal laser scanning microscope (CSLM) image series were stacked and shifted and presented as stereo pairs.

3. Results

3.1. Humic acid breakthrough

Monitoring of the head tank indicated that, after the addition of the Aldrich humic acid concentrate, this reservoir maintained a relatively steady concentration of humic acid over the next 145 days: 0.83 ± 0.06 (SD) g/l. This level was lower than the anticipated 1 g/l. Similarly, Van Stempvoort et al. (2000) reported an apparent 20% reduction in the concentration of aqueous Aldrich humic acid in standard solutions, based on total organic carbon analyses. This reduction was attributed to precipitation.

Compared to the breakthrough of bromide observed at the individual monitoring locations in the previous tracer experiment, the breakthrough of Aldrich humic acid was noticeably retarded (Fig. 3). This indicated that a significant amount of the humic acid had sorbed to the Winter Sand. Parallel batch tests reported by Van Stempvoort et al.

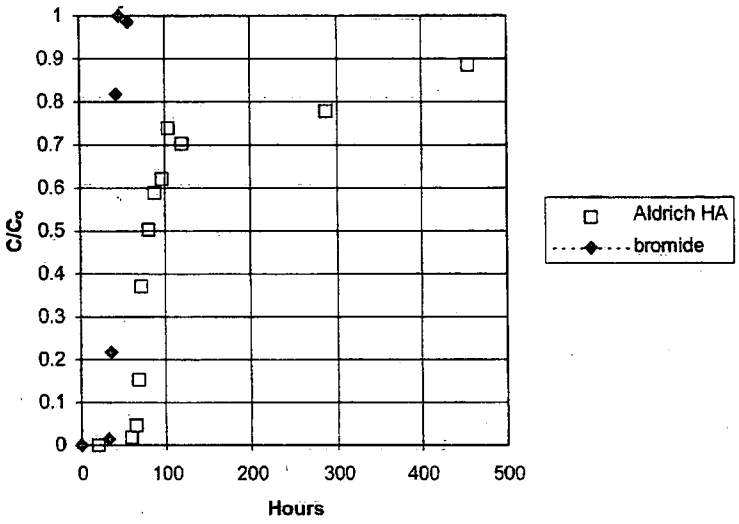

Fig. 3. Comparison of the breakthrough of the tracer bromide and of humic acid at monitoring point T2B4 (see Fig. 1 for location). Time zero is the point when either bromide or humic acid was added, in each case one pore volume is equivalent to 47 h; C is the measured concentration, and C_o is the initial concentration in the headtank.

(2000) indicated that sorption of aqueous Aldrich humic acid to the Winter Sand follows a nonlinear, Langmuir-type isotherm. Over 148 days there was a fast sorption component, and a secondary, slow sorption phase. As described in a companion paper (Molson et al., this issue), these batch data have been used to infer Langmuir sorption that includes a slow (kinetic) phase for modeling of the transport of the humic acid in this pilot scale test.

3.2. Flushing of BTEX

After emplacement of the diesel source, BTEX compounds were not detected in the air samples taken from the shallow vadose zone in the treatment cell, nor were BTEX detected in the water samples obtained from monitoring levels 1 to 3, above the diesel source. These results indicate that vertical transport of volatile diesel components, via volatilization or LNAPL migration, was apparently negligible.

As anticipated, a hydrocarbon contaminant plume developed downgradient of the diesel source at monitoring level 4. Trends in the concentrations of BTEX compounds over time in level 4 in the treatment cell are shown in Figs. 4 and 5. The concentrations of benzene detected in row 3 (depth 4), immediately downgradient of the diesel source, were always much lower than the hypothetical initial equilibrium for water in contact with the diesel source (Table 2). In contrast, the highest concentrations of toluene, ethyl-benzene and *m*- and *p*-xylenes that were detected in row 3 were close to hypothetical equilibrium (Table 2).

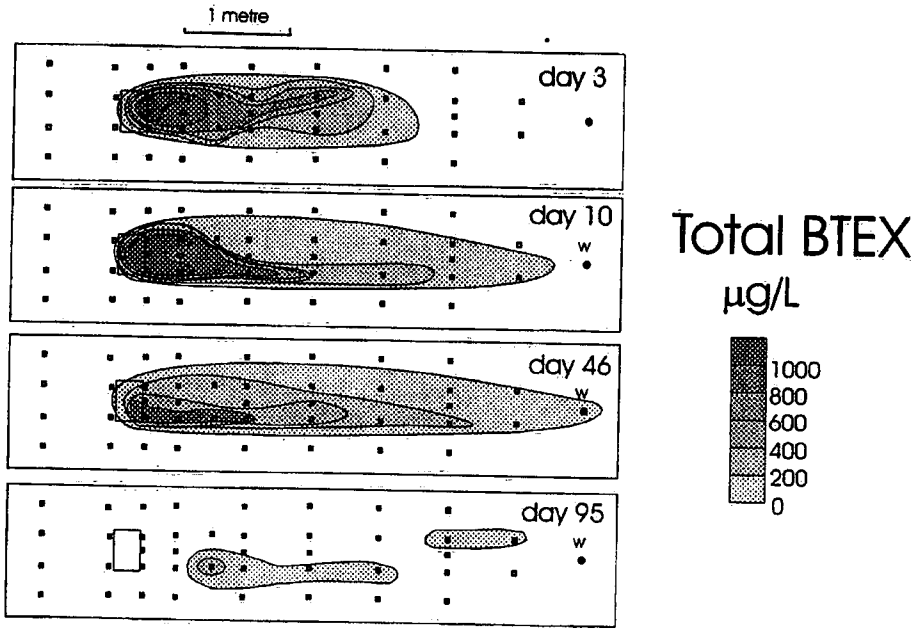

Fig. 4. Plan views of treatment cell (Fig. 1) showing trends in BTEX concentrations over time, level 4. Time is given in days after source emplacement.

Benzene, which is the most water-soluble BTEX compound (Table 2), was completely removed from the diesel source within 20 days following the source emplacement. The highest levels of benzene (39 to 54 µg/l) were observed on day 3 in monitor rows 6 and 7, approximately 1 to 2 m downgradient of the diesel source. By day 24, benzene had declined below detection at all monitoring points (e.g., Fig. 5). Based on the average linear velocity of water in the model aquifer (2 cm/h) and the length of the diesel source parallel to water flow (20 cm), and assuming that biological clogging in the source area was negligible, one pore volume of water flowed through the diesel source every 10 h. By this definition, benzene was flushed from the diesel by ~ 50 source pore volumes. In the above calculation, the source pore volume is only ~ 0.2% of the total pore volume of the treatment flow cell. Note that the residence time for water in the flow cell (5.5-m long) was 275 h.

Toluene was completely flushed from the diesel by approximately 40 days (~ 100 source pore volumes). Thus, both benzene and toluene were no longer detectable in the contaminant plume at the time the Aldrich humic acid was introduced to the head tank, 51 days after emplacement of the diesel source.

The less soluble ethylbenzene and xylenes were dissolved more slowly from the diesel source. At day 51, when the Aldrich humic acid was added to the head tank, quantities of ethyl-benzene and xylenes remained in the source. This is shown by the elevated concentrations of these compounds at the three monitoring points in row 3 (depth 4) along the downgradient edge of the source on day 45: 100 to 254 µg/l ethylbenzene and 145 to 500 µg/l xylenes. Based on previous bench-scale studies with aqueous Aldrich humic acid

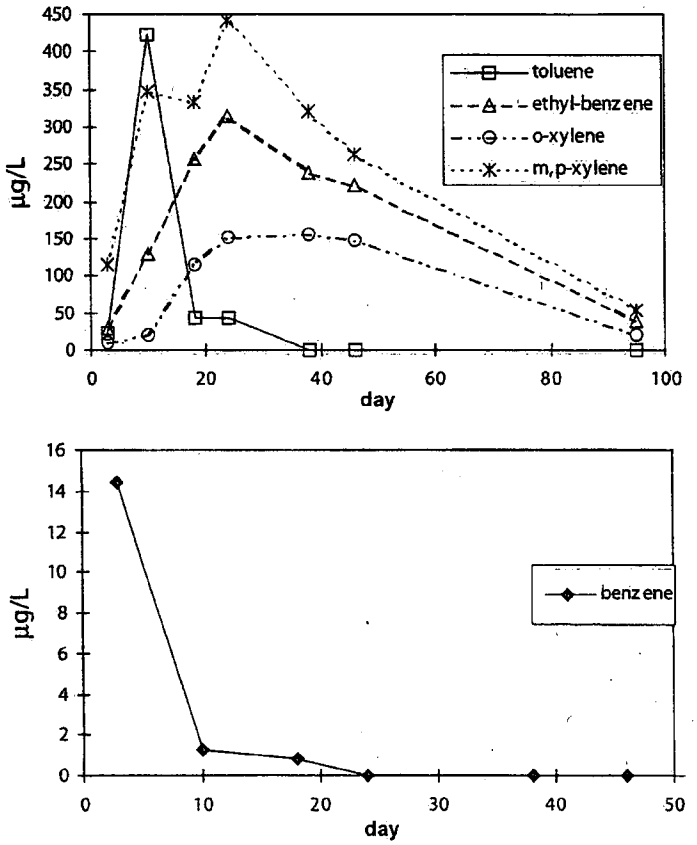

Fig. 5. Trends in levels of BTEX at monitoring point T6B4 (see Fig. 1 for location). Aldrich humic acid was added on day 51.

and gasoline (Xu et al., 1994), the addition of humic acid had little impact on the flushing of these relatively soluble aromatic compounds from the diesel source. By 95 days after source emplacement (~ 230 source pore volumes), the ethyl-benzene and xylenes had apparently been completely removed from the diesel; they were not detectable in monitoring rows 3 and 4, and only small amounts were still present in the plume (Fig. 4).

The concentrations of BTEX compounds measured over time at monitoring points in row 3 and row 9 were compiled in order to calculate mass balances for these aromatic compounds as they were transported within the contaminant plume in the model aquifer (Table 2). For the mass balance calculations, it was assumed that:

(i) the effective cross-sectional area of the plume emanating from the diesel source was equal to the rectangular cross-sectional area of the source, measured perpendicular to water flow (40 × 25 cm), times the porosity (0.3); and

(ii) for each time step, uniform levels of each BTEX compound were present in three sub-zones of the plume, corresponding to the nearest monitoring point (T3B4, T3M4 or T3C4 for row 3; T9B4, T9M4 and T9C4 for row 9), and the closest sampling event.

The mass balances shown in Table 2 indicate that less than half (~ 2% to 45%) of the BTEX that were originally present in the diesel source were detected over time in monitoring row 3, immediately downgradient of the source. Given the evidence that losses by volatilization were not significant (see above), these mass balance data suggest that large fractions of the BTEX compounds were biodegraded at the diesel source, before reaching row 3. At the source, benzene was particularly susceptible to biodegradation, and *o*-xylene was apparently also more susceptible to degradation than the other compounds.

At row 9, a molecule within the diesel plume had travelled ~ 0.7 of the distance between row 3 and the withdrawal well at the end of the cell. Based on the data in Table 2 for benzene, toluene and ethyl-benzene, only ~ 5% to 10% of the total mass of each of these compounds that was detected at row 3 was also detected at row 9. We infer that the bulk of the mass of each of these compounds was biodegraded within the model aquifer, as the plume flowed from row 3 to row 9. The xylenes were apparently degraded at slower rates within the plume, particularly the *m*- plus *p*-xylene fraction, where ~ 50% of the mass that passed row 3 was also detected at row 9.

There are no dissolved oxygen data available for this early phase (95 days) of the test. We suspect that the BTEX compounds were biodegraded by aerobic microorganisms, in spite of the fact that the pore space was initially purged with He, and that the head tank was sparged with N_2. The He purging may not have eliminated all of the air in the pore space of the model aquifer. Furthermore, air would have re-entered the pore space during the dewatering associated with source emplacement, and it is likely that residual, trapped air was present throughout the model aquifer for some time after the Winter Sand was re-saturated. Also, N_2 bubbling in the head tank probably did not remove all of the dissolved O_2. In unpublished bench scale tests (J. Lawrence), sparging of water with He or N_2 alone does not influence the redox potential, and levels of dissolved O_2 remain at ~ 0.5 mg/l.

Sulfate may have also been an important electron acceptor during biodegradation, given that the initial concentration of this anion in the tap water was 36 mg/l. The microbial analyses (Section 3.4) support this hypothesis. Other dissolved-phase electron acceptors such as nitrate (not detected), Fe (0.008 to 0.011 mg/l) and Mn (0.001 to 0.013 mg/l) were at low initial concentrations in the tap water, head tank and water sampled from the model aquifer before the tracer experiment. However, a level of 1.4 mg/l nitrate was later detected in a tap water sample. The role that mineral-phase electron-acceptors, such as Fe and/or Mn oxides, may have played as in the biodegradation of hydrocarbons is unknown.

3.3. Enhanced solubilization and transport of methylated naphthalenes (PAHs)

After the flushing of BTEX, the relatively hydrophobic MNs remained as persistent and abundant PAHs in the pilot study diesel plume. As expected, the addition of the Aldrich

Table 2
Solubility and mass balance data for BTEX in the diesel source and contaminant plume in the model aquifer

	Benzene	Toluene	Ethylbenzene	*o*-xylene	*m,p*-xylene
BTEX solubility					
Aqueous solubility (pure phase), mg/l[a]	1770	530	169	173	170
μg/g in diesel source	167	968	1104	1576	2990
Estimated mole fraction in Diesel[b] ($\times 10^3$)	0.536	2.63	2.60	3.71	7.04
Ideal water solubility from diesel (μg/l) (Raoult's Law)	949	1392	447	642	1197
Highest concentration (μg/l) detected in row 3, level 4, treatment cell	10	953	385	350	809
BTEX mass balance					
Mass (g) in diesel source at start-up	0.08	0.46	0.53	0.75	1.43
Mass (g) detected in monitoring row 3 over experiment	0.0014	0.18	0.25	0.16	0.31
Mass (g) detected in monitoring row 9 over experiment	0.00008	0.014	0.015	0.025	0.16

[a] Recommended or "best" values; Shaw (1989a,b); value for *m, p*-xylene is average.
[b] Assuming average molar weight of diesel components = 250 g.

humic acid to the water resulted in an enhanced solubilization of the MNs. As indicated by the analyses of samples collected at monitoring point T3B4, at the downgradient edge of the diesel source, the increase in total concentration of MNs on addition of the humic acid was four- to fivefold (Fig. 6). The increase was approximately twofold for the relatively soluble methylnaphthalene (Table 3), fourfold for dimethylnaphthalene and tenfold for the least soluble trimethylnaphthalene (Fig. 6). These increases in aqueous concentrations of MNs occurred as a result of the binding of these PAHs to the aqueous humic acid (Van Stempvoort and Lesage, in press).

MNs were detected at the withdrawal well on only a few occasions (5 of 35 samples), all within the first year of the experiment. By approximately 150 days after the source emplacement (i.e., 100 days after the addition of the humic acid), the plume of contaminant MNs that formed downgradient of the diesel source had reached a relatively stable configuration of ~ 0.5 m in lateral extent and ~ 3.5 m in length, and then held this approximate configuration for more than a year (Fig. 7). It appears that biodegradation had produced a "dynamic steady state" of contaminant concentrations. This condition is often reported in field studies of hydrocarbon contaminant plumes in aquifers (Chapelle, 1999). At dynamic steady state, the average rate of biodegradation of a contaminant within the

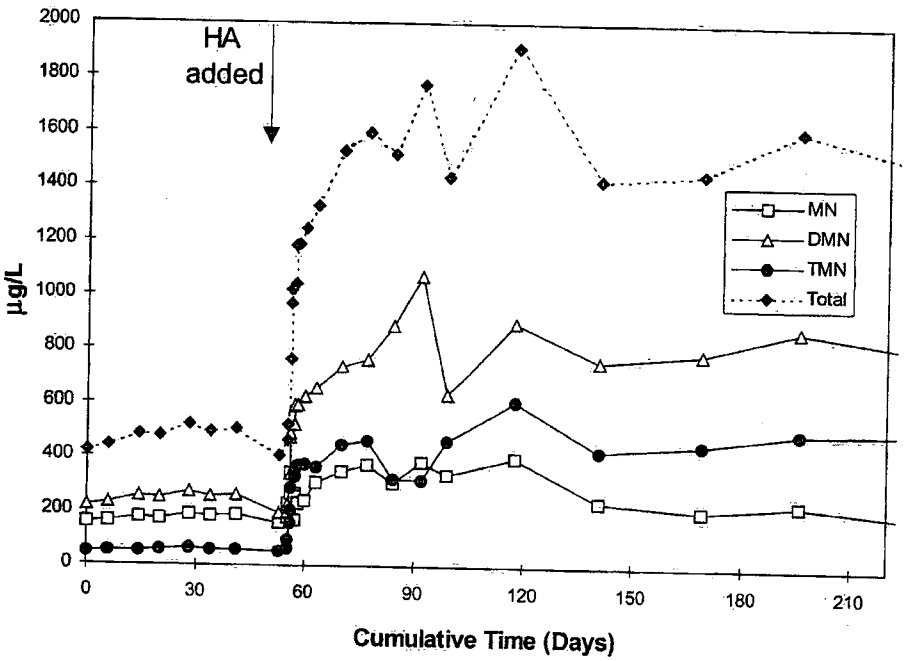

Fig. 6. Trends in levels of methylated naphthalenes at a monitoring point immediately downgradient of the diesel source (at T3B4, see Fig. 1 for location). MN = methylnaphthalene, DMN = dimethylnaphthalene, TMN = trimethylnaphthalene. Aldrich humic acid was added on May 25, 1995.

Table 3
Data on aqueous solubilities of methylated naphthalenes

Isomer	Aqueous solubility (S_w, mg/l); literature (20–25 °C)
1-Methylnaphthalene	25.8[1], 27[5], 28.5[2], 30.0[6], 30.2[3], 32.0[3]
2-Methylnaphthalene	22.6[6], 24.6[1], 25.4[2], 26[5]
1,3-Dimethylnaphthalene	8.0[2], 8.2[6]
1,4-Dimethylnaphthalene	9.5[4], 11.4[2]
1,5-Dimethylnaphthalene	2.7[1], 3.4[2]
2,3-Dimethylnaphthalene	2.0[1], 3.0[2]
2,6-Dimethylnaphthalene	1.3[1], 2.0[2]
Five other isomers	no data available
1,4,5-Trimethylnaphthalene	2.1[2]
Thirteen other isomers	no data available

(1) Eganhouse and Calder (1976); (2) Mackay and Shiu (1977); (3, 4) Burris and MacIntyre (1986, 1987); (5) Chen et al. (1994); (6) Van Stempvoort and Lesage (in press).
For additional data, see Mackay et al. (1992).

aquifer is essentially equal to its dissolution rate at the source. The overall extent and shape of the plume is dependent on the biodegradation rate, which may vary spatially. Other factors, such as retardation due to sorption, also play a role.

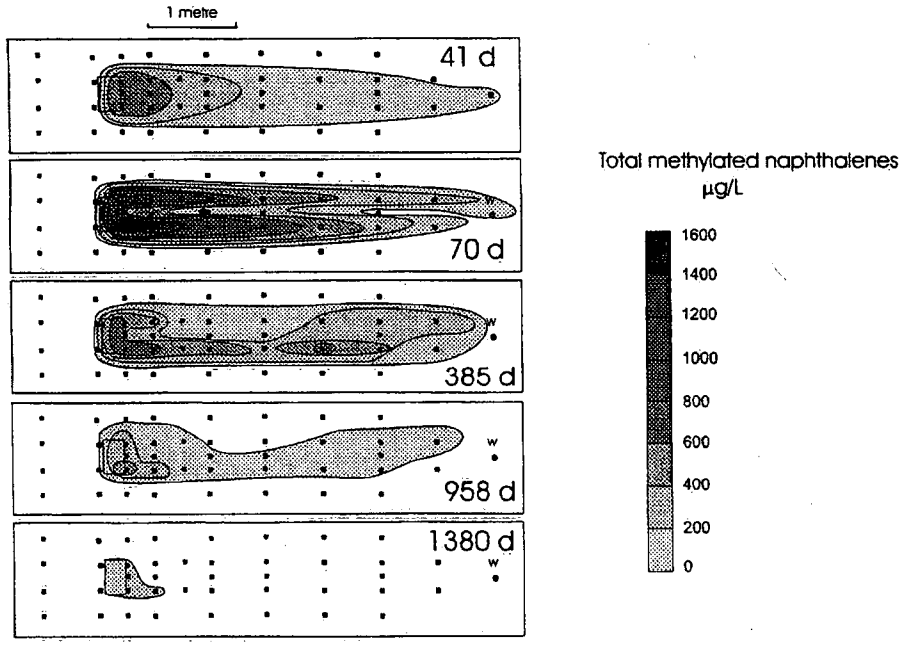

Fig. 7. Methylated naphthalene plume in treatment cell (Fig. 1) over time, level 4. Note that the top panel (41 days) represents the plume 10 days prior to HA addition; the second panel (70 days) represents the plume 19 days after HA addition.

Figs. 8–10 provide detailed information on the trends in concentrations of MNs over time at the diesel source (T3B4), in the middle (T6B4), and at the downgradient end of the model aquifer (T9B4), respectively. These data illustrate the sequential flushing of PAHs over time. The sequential disappearance of the methylated naphthalene groups was related to their water solubility. The relatively soluble MN was flushed out first, followed by DMN, and finally the least soluble TMN.

The shape of the plume (Fig. 7) and the breakthrough trends in concentrations of MNs (Figs. 8–10) were not always smooth. At 70 days, the plume appeared to be split into two main zones (Fig. 7). The levels of MNs at each point within the plume fluctuated up and down to some extent over time. Some of the MNs exhibited more than one major peak in concentration (Figs. 9 and 10). The origin of these spatial and temporal complexities is uncertain. However, they indicate that either the flow system or the decay of the contaminants varied spatially or temporally. The complexities in the plume concentrations may be related to the eventual development of a heterogeneous flow system within the model aquifer, due to localized biological clogging (Baveye et al., 1998), associated with in situ bioremediation of the diesel contaminants. This hypothesis is supported by the microbial analyses (Section 3.4), which indicated the presence of biofilms and elevated

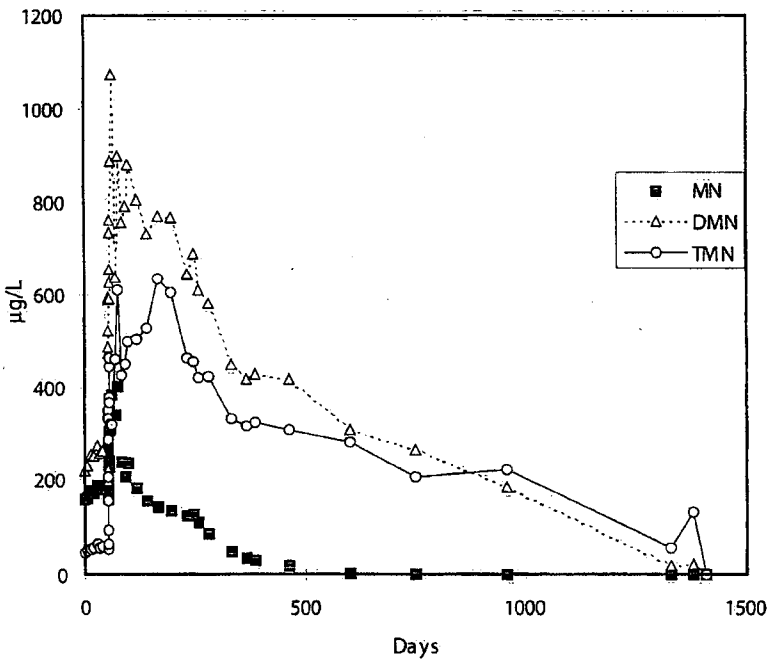

Fig. 8. Changes in methylated naphthalene concentrations at T3B4 (see Fig. 1 for location, immediately downgradient of diesel source) over time, showing the sequential depletion of methylnaphthalene (MN), followed by dimethylnaphthalene (DMN), and then trimethylnaphthalene (TMN).

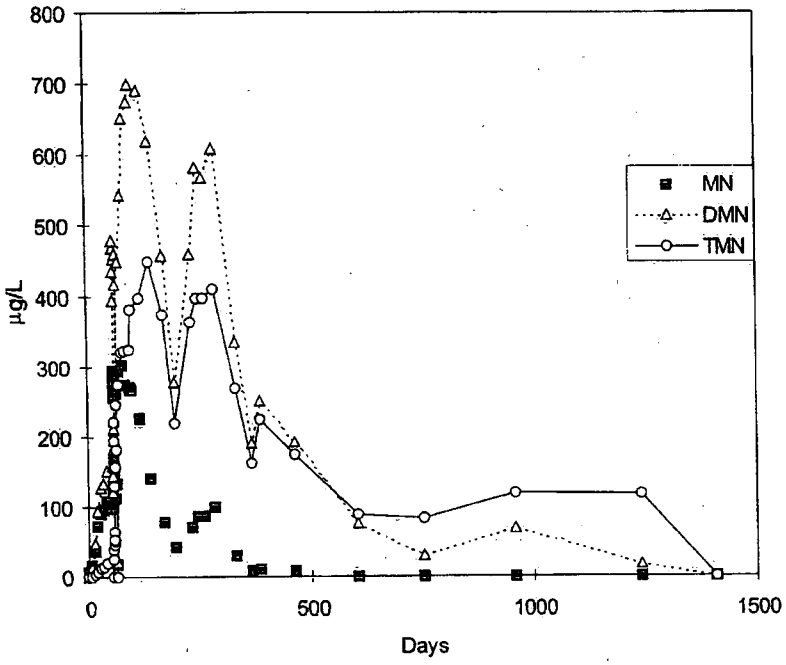

Fig. 9. Changes in methylated naphthalene concentrations at T6B4 (see Fig. 1 for location) over time. As in Fig. 11, note the sequential depletion of MN, followed by DMN, and then TMN.

concentrations of bacteria in the samples of the diesel source that were collected at the end of the experiment (Figs. 11 and 12).

Despite the above spatial and temporal fluctuations, the overall pattern of plume shape and decay over time is relatively straightforward. Approximately 1 year after the source emplacement, the total concentration of MNs in the contaminant plume began to decline noticeably. At ~ 380 days after the source emplacement, the toxicity of the diesel plume was assessed using the Microtox™ test. The results indicated a very strong correlation between total methylnaphthalene concentrations and toxicity (data not shown).

By 600 days (~ 1400 source pore volumes: see Section 3.2), the methylnaphthalene (MN) had declined throughout the plume to levels that were below 10 µg/l, due to flushing from the source (Figs. 8–10). The remaining plume, consisting of DMN and TMN, shrank in size, and was no longer detectable (< 5 to 10 µg/l each) at some of the monitoring points in rows 6 through 10. After approximately 4 years (~ 3500 source pore volumes) following source emplacement, the methylated naphthalene plume had virtually disappeared, as DMN and TMN were no longer detectable throughout the treatment side of the model aquifer (Figs. 7–10). At the end of the experiment (~ 5 years after source emplacement), the total diesel hydrocarbons in the source had decreased substantially. Based on total petroleum hydrocarbon analyses of core and porewater samples collected at this time, less than 4% of the diesel mass in the source remained.

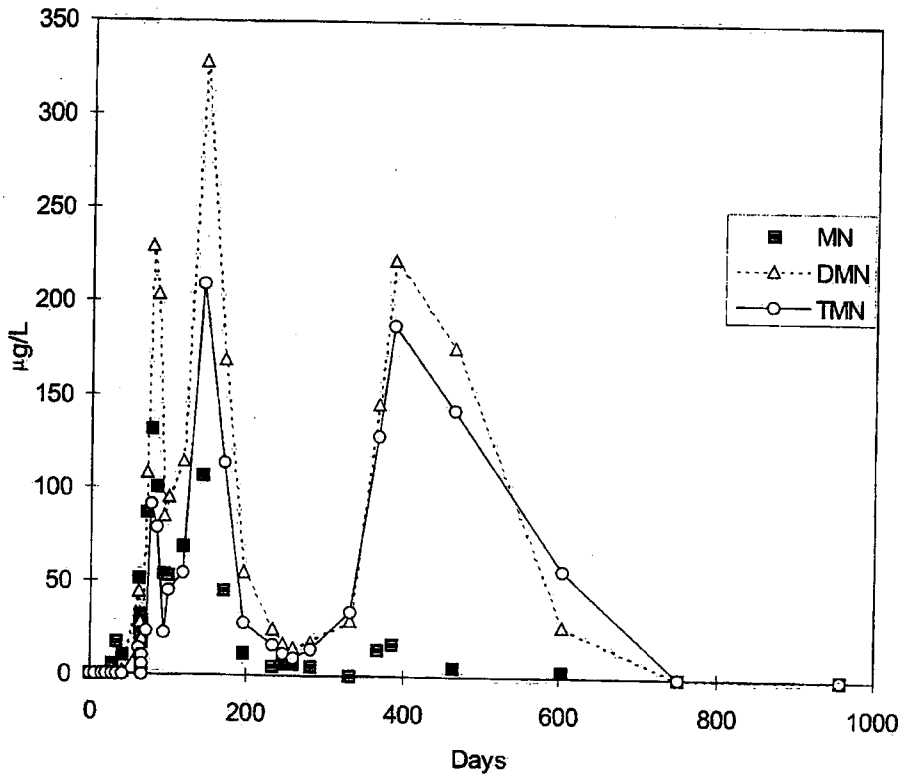

Fig. 10. Changes in methylated naphthalene concentrations at T9B4 (see Fig. 1 for location) over time. Note the preferential depletion of MN, and strong second peaks in concentrations of DMN and TMN.

Dissolved oxygen measurements, taken at approximately 3.5 years after source emplacement, indicated that downgradient of the source, the diesel plume in the treatment cell was largely anaerobic, whereas the surrounding zones and the control cell remained aerobic. These data suggest that aerobic biodegradation of hydrocarbons was an important process within and/or in the immediate vicinity of the diesel source. This interpretation is consistent with the microbial analyses (Section 3.4), which indicated that biofilms had developed on the sediment at the diesel source. It is likely that the available dissolved O_2 limited the overall rate of aerobic biodegradation of hydrocarbons at the source, and also limited the biodegradation of MNs in the plume. This may have controlled the configuration of the "steady state" plume within the model aquifer. Anaerobic bacteria may also have contributed to the diesel biodegradation process (cf. Sections 3.2 and 3.4).

Similar to the mass balance approach for BTEX (Section 3.2), the concentrations of MNs measured over time at monitoring points in row 3 and row 9 were compiled in order to estimate the total amounts of these PAHs that were detected at each of these rows over

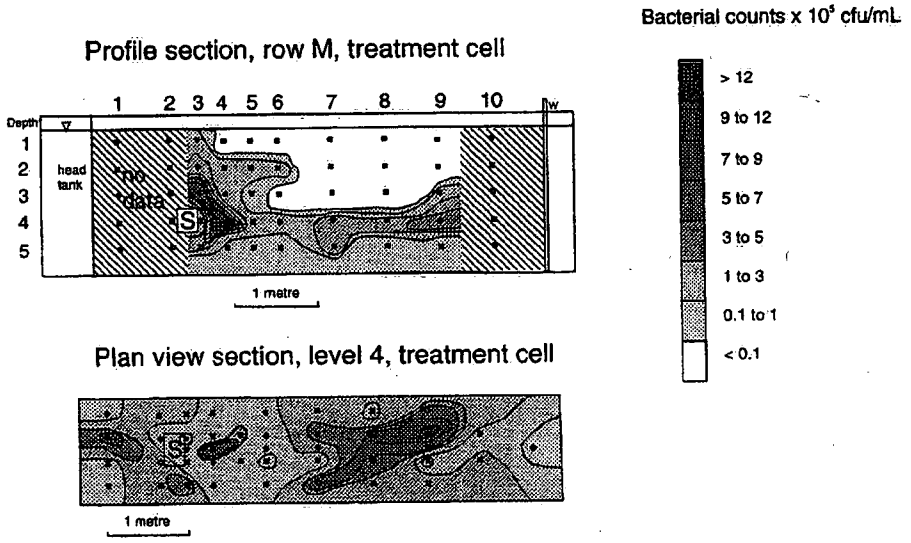

Fig. 11. Distribution of bacteria at 400 days, based on plate counts. Diesel source is indicated as "S".

time. The total amounts of methylated naphthalenes that were detected in row 3, just downgradient of the diesel source, were very similar to those present in the source at startup (Table 4). Thus an approximate mass balance for MN, DMN and TMN was achieved in the pilot experiment. Also, this mass balance indicates that biodegradation of these PAHs within the diesel source was not an important process.

A comparison of the row 3 and row 9 data (Table 4) indicates that approximately 70% to 80% of the methylated naphthalenes that were detected at row 3 had biodegraded by the time the plume reached row 9 (a horizontal distance of 2.9 m). Based on the same mass balance approach, less than half a percent of each of the MNs that were leached from the source were detected at the withdrawal well for the treatment cell (data not shown). However, this is a conservative estimate of the breakthrough at the withdrawal well, because considerable dilution of the plume occurred during mixing in this well ($\sim 20\times$), and breakthroughs of low levels of MNs (<5 to 10 μg/l each) would not be detected.

3.4. Microbial analyses

Plate count analyses of bacteria in the system at day 400 indicated a complete colonization of level 4 of the treatment cell (Fig. 11). Bacterial counts were generally on the order of 2 to 5×10^5 cfu/ml with no specific trend across the system. Samples T4M4 and T9C4, however, had counts an order of magnitude higher, 1.24×10^6 and 1.86×10^6 cfu/ml, respectively. The vertical distribution indicated that bacteria were more concentrated at level 4 across the length of the treatment side, except in row 3, just downstream of the source, where concentrations were elevated at all depths (Fig. 11). Notably high biomass concentrations were obtained from samples T3M3 (1.12×10^6 cfu/

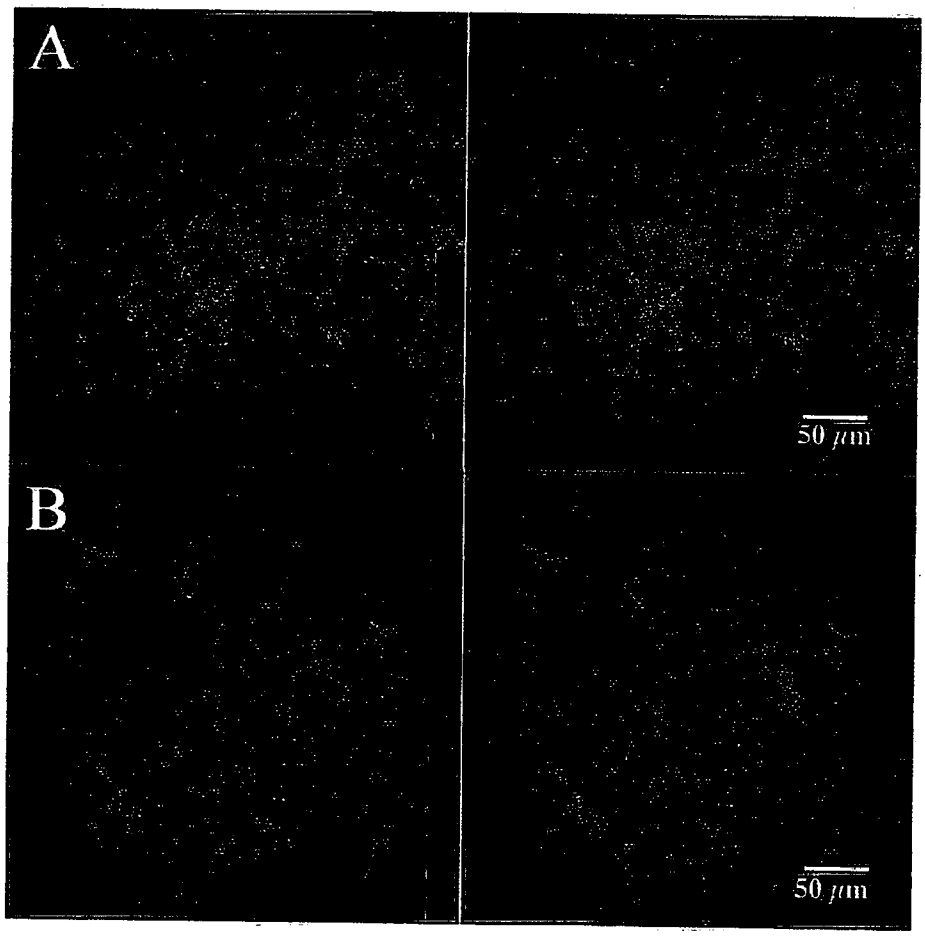

Fig. 12. Stereo pair images of diesel source samples by confocal laser scanning microscopy. Bacterial cells and aggregates are stained green (Syto9); zones stained red and blue are various exopolymeric materials that bound the fluor-conjugated lectins *Triticum vulgaris* TRITC (red) and *Tetragonolobus purpureas* CY5 (blue). (A) Fine sediment grains that were suspended in a water sample, coated with a biofilm (20–50 μm) consisting of exopolymer and bacterial cells. (B) Image of an entire sand grain covered with a thin (10–40 μm) biofilm.

ml) and T4M4 (1.24×10^6 cfu/ml). At this point in the study, bacteria were almost nonexistent in the control cell with most of the samples (12 of 13) producing zero to only a few colonies. Only one sample yielded a significant number of colonies, C6C4, with a count of 4.0×10^5 cfu/ml. These lateral and vertical distributions of bacteria indicate that microbial growth was strongly related to the presence of the diesel source. The generally higher levels downgradient of the source at level 4 reflect the observed active biodegradation within the diesel contaminant plume (Fig. 11).

Table 4
Total masses of methylnaphthalene (MN), dimethylnaphthalene (DMN) and trimethylnaphthalene (TMN): (1) in the diesel source at start-up; (2) detected in row 3 over time; and (3) detected in row 9 over time, based on HPLC analyses

Total masses, methylated naphthalenes	MN (g)	DMN (g)	TMN (g)
(1) In Diesel Source	0.80	4.53	4.43
(2) Detected in row 3 (T3B4, T3M4 and T3C4)	0.67	5.08	4.47
(3) Detected in row 9 (T9B4, T9M4 and T9C4)	0.18	1.20	1.27

The microscopic observations of stained samples, collected from the diesel source on completion of the experiment, indicated that biofilms had developed on the surfaces of the grains of Winter Sand (Fig. 12). The biofilms have some relief, extending out 50+ μm from the grain surfaces. This is direct evidence for potential bioclogging, which may have reduced hydraulic conductivity within the diesel source during the course of the experiment. Diesel droplets were not observed in these samples, apparently due to almost complete degradation of the source. Microbial colonization of diesel droplets has been described previously (Paulsen et al., 1999; Whyte et al., 1999), and may have been present earlier in the study.

Core samples of the Winter Sand were analyzed by molecular techniques to provide details regarding the microbial strains that had colonized the model aquifer. Unfortunately, purified DNA could not be obtained, due to the high concentration of humic acid, which is a known inhibitor of DNA isolation and purification (Tebbe and Vahjen, 1993). In contrast, the phospholipid fatty acid extraction analyses are unaffected by the presence of humic acids. These analyses provide information about microbial biomass, physiology and to a certain extent, taxonomy (Green and Scow, 2000). For three samples collected at the end of the experiment, viable biomass, as measured by total PLFAs extracted, indicated that microbial concentrations were highest in the diesel source (Table 5). Bacteria had colonized both treatment and control cells, resulting in quite similar biomass concentrations between rows 4 and 5 in each cell (Table 5). This was probably due to the recirculating nature of the system, whereby bacteria that grew in response to the presence of the diesel contaminants in the treatment cell were carried via the water to inoculate the control side. In contrast, for the water samples collected at 400 days (see above), significantly different plate counts were observed in the treatment and control cells.

As assessed by the distribution of lipid biomarkers, the samples contained relatively diverse microbial populations, representing several specific groups of bacteria (Table 5). High proportions of monoenoic PLFAs (Monos) in all three samples, specifically 16:1ω7c, 18:1ω7c, and cy19:0, suggest populations dominated by gram-negative bacteria. Generally fast growing and adaptive bacteria, gram-negative species are common to hydrocarbon contaminated sites (MacNaughton et al., 1999; Ringelberg et al., 1999). Langworthy et al. (1998) also observed an enrichment of 16:1ω7 and 18:1ω7 fatty acids in PAH contaminated soil, both of which were associated with aerobic, gram-negative bacteria.

Terminally branched saturated PLFAs (TerBrSats), generally found in gram-positive strains, were highest in the source sample, as were branched monoenoic (BrMono) PLFAs,

Table 5
Phospholipid fatty acid (PLFA) analyses of Winter Sand samples collected at test completion

	Control cell, rows 4–5	Treatment cell, rows 4–5	Diesel source
Total PLFAs (pmol/g)	140	195	416
Biomass (cfu/g)	2.80×10^6	3.90×10^6	8.33×10^6
Subdivisions of PLFAs, as percent of total			
Terminally branched saturated	6.8	6.0	7.7
Monoenoic	46.0	53.4	46.9
Branched monoenoic	2.6	1.7	3.2
Mid-chain branched saturated	19.1	13.4	9.7
Polyunsaturated	8.3	7.6	16.3
Nonspecific saturated	17.2	17.9	16.2
Physiological ratios			
Growth phase	2.73	1.82	0.60
Stress	0.03	0.07	0.14

A conversion factor of 2×10^4 cells/pmol PLFA was used for colony forming unit (cfu) estimations. Values for PLFA subdivisions are percent of total. Physiological measurements are ratios as discussed in the text.

representative of anaerobic sulfate or iron-reducing bacteria, and polyunsaturated PLFAs (Poly), representative of microeukaryotic organisms. In the latter group the presence of 18:2ω6 is an indicator of fungal biomass, and 20:4ω6 indicates protozoa. Proliferation of protists at contaminated sites in response to increased bacterial biomass has been reported for a number of subsurface sites (Madsen et al., 1991). Biomarkers i17:1ω7c, a branched monoenoic, and 10me16:0, a mid-chain branched saturate (MidBrSat), specific to sulfate-reducing bacteria of the genera *Desulfovibrio* and *Desulfobacter*, respectively, were present in all samples. Mid-chain branched PLFAs are common to actinomycetes and sulfate-reducing bacteria, but some are genera- or group-specific. The MidBrSat 10me18:0 of actinomycetes was found in all samples. Nonspecific saturated PLFAs (Nsats), such as 16:0 and 18:0, found in both prokaryotes and eukaryotes, comprised an average 17% of total PLFA profiles.

Generally, there was little difference between source, treatment, and control PLFA profiles, suggesting that similar communities had developed at each location by the end of the study. However, while lipid biomarkers are good qualitative indicators of microbial presence or absence, their use as quantitative indicators is more limited (Green and Scow, 2000).

The physiological status of gram-negative communities can be assessed from ratios of the various monoenoic biomarkers. Biomarkers 16:1ω7c and 18:1ω7c are converted to cyclopropyl fatty acids (cy17:0, cy19:0) as microbes move from log to stationary growth phase. Ratios cy17:0/16:1ω7c and cy19:0/18:1ω7c, when summed, usually fall within the range of 0.1 (log phase) to 5.0 (stationary phase), being inversely proportional to the turnover rate. The PLFA analyses indicate that the communities in all three samples were in the stationary phase of growth (Table 5), but bacteria at the source were found to have the fastest turnover rate, followed by those in rows 4–5 of the treatment cell, and the slowest rate was for the control cell sample. This is consistent with the available carbon at

each location and with the apparent degradative activity in the source and treatment cell. Increases in cyclopropyl PLFAs are sometimes also associated with anaerobic metabolism (personal communication: Greg Davis, Microbial Insights, Rockford, TN).

Gram-negative bacteria also generate *trans* fatty acids to minimize the permeability of their cellular membranes as an adaptation to toxic or stressful environments. This adaptation is indicated when the sum of ratios 16:1ω7t/16:1ω7c and 18:1ω7t/18:1ω7c (*trans/cis*) is greater than 0.1. The diesel source community showed evidence of stress with a *trans/cis* ratio of 0.14. The treatment cell sample taken between rows 4–5 had a higher *trans/cis* ratio (0.07) than the control cell sample (0.03), yet neither would be considered 'stressed'.

4. Discussion

4.1. Binding of methylated naphthalenes to aqueous Aldrich humic acid

As outlined above, in our pilot-scale study we observed enhanced solubilization of MNs due to binding by Aldrich humic acid, manifested as an increase in concentrations of MNs immediately downgradient of the diesel source, following the addition of humic acid. Based on a comparison of the average concentrations of MNs measured in the few weeks prior to humic acid addition to those after, the apparent coefficients ($K_{oc,\ app}$) for the binding of MNs to Aldrich humic acid were similar to those determined in concurrent bench-scale testing by Van Stempvoort and Lesage (in press) for pure phase MNs in nominal 1 g/l Aldrich humic acid (Table 6). This indicates that binding batch tests, as reported by Van Stempvoort and Lesage, can provide useful data for estimating the potential for enhanced solubilization of these and other diesel components at the pilot and/or field scale.

The $K_{oc,\ app}$ values shown in Table 6 increase as the hydrophobicity of the MNs increase: the most soluble MN has the lowest $K_{oc,\ app}$, and the least soluble TMN the highest $K_{oc,\ app}$ values. These results are consistent with previous studies, which found that the affinities of organic contaminants to aqueous humic acid are proportional to the hydrophobicities of the contaminants (McCarthy and Jimenez, 1985; Chiou et al., 1986). The $K_{oc,\ app}$ value determined by Van Stempvoort and Lesage (in press) for 2,3,5-TMN was approximately half the value for TMN (mixed isomers) based on this pilot test (Table 6), suggesting that 2,3,5-TMN may be a relatively hydrophilic member of this group of 14 isomers, and/or that another diesel component is interfering with the TMN analysis by HPLC. Unfortunately, water solubility data for various isomers of this group are not available.

4.2. Biodegradation

Our results show that biodegradation of MNs was a key process within the contaminant plume in the model aquifer, even in the presence of concentrated (0.8 g/l) Aldrich humic acid. Two different approaches to the rate of biodegradation in this experiment can be considered: the overall rate (total biodegradation per unit time), and the

Table 6
Summary of apparent binding coefficients ($K_{oc,\ app}$)

Isomer	Technique	Duration of test	$K_{oc,\ app}$ (l/kg)
1-MN	Comparative solubility[a]	1 to 12 days	$2.61\ (\pm 0.30) \times 10^3$ to $6.37\ (\pm 0.46) \times 10^3$
1-MN	SPME[a]	1 day	$2.16\ (\pm 0.45) \times 10^3$
2-MN	SPME[a]	1 day	$1.69\ (\pm 0.27) \times 10^3$
MNs	this study[b]	7 weeks	$2.74\ (\pm 1.08) \times 10^3$
1,3-DMN	comparative solubility[a]	1 to 2 days	$15.0\ (\pm 0.06) \times 10^3$ to $17.1\ (\pm 0.06) \times 10^3$
1,3-DMN	SPME[a]	1 day	$5.04\ (\pm 0.69) \times 10^3$
1,7-DMN	SPME[a]	1 day	$3.54\ (\pm 0.41) \times 10^3$
DMNs	this study[b]	7 weeks	$7.85\ (\pm 2.56) \times 10^3$
2,3,5-TMN	SPME[a]	1 day	$9.81\ (\pm 1.00) \times 10^3$
TMNs	this study[b]	7 weeks	$21.6\ (\pm 6.0) \times 10^3$

MN = methylnaphthalene; DMN = dimethylnaphthalene; TMN = trimethylnaphthalene. SPME refers to solid phase microextraction technique.

[a] Values for individual isomers: bench-scale batch tests with nominal 1g/l Aldrich humic acid (301 mg/l carbon; Van Stempvoort and Lesage, in press).

[b] Based on pilot scale study monitoring data: average concentrations in row 3, depth 4, before (by 23 to 10 days) and after (by 7 to 26 days) humic acid addition, using Eqs. (2) to (5) in Van Stempvoort and Lesage (in press). We assumed that the 0.83 g/l Aldrich HA had 301 mg/l organic carbon (as per batch test).

specific rate (biodegradation per unit time per unit volume). The results of this pilot-scale test indicate that the humic acid addition enhanced the solubilization and aqueous transport of MNs from a residual hydrocarbon source. Apparently, as a direct result of these effects, the humic acid enhanced the overall biodegradation rate of these PAHs. This conclusion is based on our inference that, during steady state, the overall biodegradation rate of MNs was directly controlled by, and equal to the dissolution rate of these MNs.

In contrast, the specific biodegradation rate of MNs at various locations within the model aquifer was likely controlled by their aqueous concentrations, and the concentrations of dissolved O_2 and bacteria. This inference is based on the fact that bacterial growth proliferated within the diesel source and an anaerobic zone developed within the plume. Perhaps other factors played a role, such as availability of other electron acceptors, nutrients, and humic acid concentrations. Our results suggest that the presence of 0.8 g/l Aldrich humic acid did not strongly inhibit the specific biodegradation rate of hydrocarbons derived from diesel. We did not examine the rate of biodegradation of MNs in the plume as a function of humic acid concentration. However, previous microcosm slurry experiments have shown that the presence of concentrated (50 to 2000 mg/l) Aldrich humic acid may have some inhibitory effect on the mineralization of pure phase PAHs, but seems to enhance the biodegradation of whole oil (Lesage et al., 1997).

In this experiment, biodegradation of hydrocarbons lowered the dissolved O_2 concentrations to trace levels in the plume downflow of the diesel source. It is possible that

bacteria were using the O_2 to selectively degrade diesel components within the immediate source area, such as BTEX (see Section 3.2), and short-chain aliphatics. Selective biodegradation of short-chain aliphatics/*n*-alkanes in diesel has been observed in batch tests (Geerdink et al., 1996; Olson et al., 1999), although the fate of PAHs specifically was not closely monitored. Such selective biodegradation could perhaps explain why the MNs were apparently completely removed by dissolution and flushed away from the source over time (given the mass balance shown in Table 4), rather than partially degraded within the source zone. We speculate that the degradation of MNs within the model aquifer may have been largely controlled by mixing of the O_2-deficient contaminant plume with aerobic water along its margins. Such oxygen-limited biodegradation has been described previously with respect to field-scale plumes of hydrocarbons (e.g., Borden et al., 1986), and is confirmed for this experiment by the numerical simulations provided in the companion paper (Molson et al., this issue). It is likely that ongoing biodegradation of slightly soluble aliphatics continued in the diesel source area after the depletion of the MNs. Our inference that the aliphatics were also degraded is supported by the TPH data collected at 5 years, indicating that less than 4% of the total diesel mass remained in the source.

4.3. Conclusions

In this pilot-scale test, a nonaqueous diesel fuel source was placed below the water table in a model aquifer. Concentrated Aldrich humic (0.83 g/l) was added to the influent water and served as a carrier (flushing agent), binding methylated naphthalenes (MNs) and enhancing their solubilization. For the various MNs, the enhancement ranged from two- to tenfold, increasing with hydrophobicity: methylnaphthalene > dimethylnaphthalene > trimethylnaphthalene. As anticipated, this enhanced solubilization process resulted in an accelerated removal of these compounds from the diesel source. In contrast, the addition of the humic acid did not have a significant effect on the solubilization of the more hydrophilic BTEX compounds.

Over the course of the experiment, the amounts of MNs and BTEX removed from the diesel source were monitored immediately downgradient. Calculations based on these data indicated that the amounts of MNs removed from the diesel source were very similar to the amounts inferred to be present in the source at startup. Thus, a mass balance for these PAHs was realized.

The monitoring of the concentrations of MNs and BTEX at points further downgradient from the source indicated that the bulk of these compounds were biodegraded within the model aquifer, prior to removal of the water at the extraction well 4 m downgradient of the diesel source. In the case of the MNs, this result suggests that the addition of the humic acid resulted in an accelerated in-situ bioremediation, directly related to their enhanced solubilization. Depleted O_2 within the contaminant plume suggests that aerobic biodegradation was dominant in this system. The microbial analyses indicate that some anaerobes were also present, but their significance is uncertain.

Given the positive results of this experiment, it will be useful to consider higher concentrations of aqueous humic acid in future tests at the pilot scale. Recent bench-scale experiments (Johnson and John, 1999; Boving and Brusseau, 2000; Van Stempvoort and

Lesage, in press) suggest that higher levels of humic acid, ranging from 10 g/l to 5% by weight, would result in even more efficient flushing of organic contaminants present as (a) nonaqueous phase(s) in groundwater.

Acknowledgements

The authors wish to thank the Panel for Energy Research and Development (PERD), the National Energy Board and Environment Canada for their support. Thanks also to Imperial Oil of Canada for their gift of diesel fuel samples. Sincere thanks to Dr. Carl Enfield of the U.S. EPA R. S. Kerr laboratory in Ada, OK for invaluable advice on the instrumentation and filling of the tank. The technical assistance of Jerry Ford, John Voralek, Rob Hoag, Louise Durham, Mark Flumiani, Bryan Helfenbaum, Charles Talbot, John Fitzgerald, Greg Bickerton, Dianne Thompson, Michael Venhuis, Bryan Taylor, Dan Banks, Tomas Chihula and Jamie Burkell has made this project possible. The manuscript was improved by the comments of William P. Johnson and an anonymous reviewer.

References

Abdul, A.S., Gibson, T.L., Rai, D.N., 1990. Use of humic acid solution to remove organic contaminants from hydrogeologic systems. Environ. Sci. Technol. 24, 328–333.

American Public Health Association, 1995. In: Eaton, A.D., Clesceri, L.S., Greenberg, A.E. (Eds.), Standard Methods for the Examination of Water and Wastewater, 19th edn. Washington, DC.

Barkay, T., Navon-Venezia, S., Ron, E.Z., Rosenberg, E., 1999. Enhancement of solubilization and biodegradation of polyaromatic hydrocarbons by the bioemulsifier alasan. Appl. Environ. Microbiol. 65, 2697–2702.

Baveye, P., Vandevivere, P., Hoyle, B.L., DeLeo, P.C., Sanchez de Lozada, D., 1998. Environmental impact and mechanisms of the biological clogging of saturated soils and aquifer materials. Crit. Rev. Environ. Sci. Technol. 28, 123–191.

Bettahar, M., Schäfer, G., Baviére, M., 1999. An optimized surfactant formulation for the remediation of diesel oil-polluted sandy aquifers. Environ. Sci. Technol. 33, 1269–1273.

Borden, R.C., Bedient, P.B., Lee, M.D., Ward, C.H., Wilson, J.T., 1986. Transport of dissolved hydrocarbons influenced by oxygen-limited biodegradation: 2. Field application. Water Resour. Res. 22, 1983–1990.

Boving, T.B., Brusseau, M.L., 2000. Solubilization and removal of residual trichloroethene from porous media: comparison of several solubilization agents. J. Contam. Hydrol. 42, 51–67.

Brubaker, G.R., 1991. In situ bioremediation of PAH-contaminated aquifers. Proceedings of the Petroleum Hydrocarbons and Organic Chemicals in Ground Water: Prevention, Detection and Restoration Conference, Nov. 20–22, Houston, Texas. Groundwater Management, Dublin, Ohio, pp. 377–390.

Burkhard, L.P., 2000. Estimating dissolved organic carbon partition coefficients for nonionic organic chemicals. Environ. Sci. Technol. 34, 4663–4668.

Burris, D.R., MacIntyre, W.G., 1986. A thermodynamic study of solutions of liquid hydrocarbon mixtures in water. Geochim. Cosmochim. Acta 50, 1545–1549.

Burris, D.R., MacIntyre, W.G., 1987. Water solubility behavior of hydrocarbon mixtures—implications for petroleum dissolution. In: Vandermeulen, J.H., Hrudey, S.E. (Eds.), Oil in Freshwater: Chemistry, Biology, Countermeasure Technology. Proceedings of the Symposium of Oil Pollution in Freshwater, Edmonton, AB, Canada. Pergamon Press, New York, pp. 85–94.

Chapelle, F.H., 1999. Bioremediation of petroleum hydrocarbon-contaminated ground water: the perspectives of history and hydrology. Ground Water 37, 122–132.

Chen, C.S.-H., Delfino, J.J., Rao, P.S.C., 1994. Partitioning of organic and inorganic components from motor oil into water. Chemosphere 28, 1385–1400.

Chiou, C.T., Malcolm, R.L., Brinton, T.I., Kile, D.E., 1986. Water solubility enhancement of some organic pollutants and pesticides by dissolved humic and fulvic acids. Environ. Sci. Technol. 20, 502–508.

Eganhouse, R.P., Calder, J.A., 1976. The solubility of medium molecular weight aromatic hydrocarbons and the effects of aromatic hydrocarbon co-solutes and salinity. Geochim. Cosmochim. Acta 40, 555–561.

Falta, R.W., 1998. Using phase diagrams to predict the performance of cosolvent floods for NAPL remediation. Ground Water Monit. Rem., 94–102 (Summer).

Geerdink, M.J., van Loosdrecht, M.C.M., Luyben, K.C.A.M., 1996. Biodegradability of diesel fuel. Biodegradation 7, 73–81.

Green, C.T., Scow, K.M., 2000. Analysis of phospholipid fatty acids (PLFA) to characterize microbial communities in aquifers. Hydrogeol. J. 8, 126–141.

Johnson, W.P., John, W.W., 1999. PCE solubilization and mobilization by commercial humic acid. J. Contam. Hydrol. 35, 343–362.

Krop, H.B., Paul, C.M., Govers, H.A.J., 2001. Determination and theoretical aspects of the equilibrium between dissolved organic matter and hydrophobic organic micropollutants in water (K_{doc}). Rev. Environ. Contam. Toxicol. 169, 1–122.

Langworthy, D.E., Stapleton, R.D., Sayler, G.S., Findlay, R.H., 1998. Genotypic and phenotypic responses of a riverine microbial community to polycyclic aromatic hydrocarbon contamination. Appl. Environ. Microbiol. 64, 3422–3428.

Lee, L.S., Hagwall, M., Delfino, J.J., Rao, P.S.C., 1992. Partitioning of polycyclic aromatic hydrocarbons from diesel fuel into water. Environ. Sci. Technol. 26, 2104–2110.

Lesage, S., Xu, H., Novakowski, K.S., Brown, S., Durham, L., 1995. Use of Humic Acids to Enhance the Removal of Aromatic Hydrocarbons from Contaminated Aquifers: Part II. Pilot Scale. Fifth Annual Symposium on Groundwater and Soil Remediation, Toronto, Ontario October 2–6. Environmental Protection Service, Environment Canada, Hull, Canada, Proceedings on CD/ROM, 10 pp.

Lesage, S., Hofmann, H., Li, W.-C., Millar, K., Liu, D., Seidel, H., 1997. Effect of humic acids on the biodegradation of PAHs by bacteria and fungi. In: Alleman, B., Leeson, A. (Chairs), In Situ and On-Site Bioremediation, Proceedings of the Fourth International Symposium on In Situ and On Site Bioremediation. New Orleans, Louisiana, April 28–May 1, 1997, vol. 4(2) pp. 185–191.

Lesage, S., Novakowski, K.S., Brown, S., Millar, K., 2001. Humic acids enhanced removal of aromatic hydrocarbons from contaminated aquifers: developing a sustainable technology. Special Issue of J. Environ. Sci. Health, Part A: Toxic/Hazard. Subst. Environ. Eng. A36, 1515–1533.

Mackay, D., Shiu, W.Y., 1977. Aqueous solubility of polynuclear aromatic hydrocarbons. J. Chem. Eng. Data 22, 399–402.

Mackay, D., Shiu, W.Y., Ma, K.C., 1992. Illustrated Handbook of Physical–Chemical Properties and Environmental Fate for Organic Chemicals, vol. II. Lewis Publishers, Chelsea, MI, USA.

MacNaughton, S.J., Stephen, J.R., Venosa, A.D., Davis, G.A., Chang, Y.-J., White, D.C., 1999. Microbial population changes during bioremediation of an experimental oil spill. Appl. Environ. Microbiol. 65, 3566–3574.

Madsen, E.L., Sinclair, J.L., Ghiorse, W.C., 1991. In situ biodegradation: microbiological patterns in a contaminated aquifer. Science 252, 830–833.

Martel, R., Gélinas, P.J., 1996. Surfactant solutions developed for NAPL recovery in contaminated aquifers. Ground Water 34, 143–154.

Martel, K.E., Martel, R., Lefebvre, R., Gélinas, P.J., 1998. Laboratory study of polymer solutions used for mobility control during in situ NAPL recovery. Ground Water Monit. Rem., 103–113.

Mas-Pla, J., Jim Yeh, T.-C., McCarthy, J.F., Williams, T.M., 1992. Numerical simulation of a two-well tracer experiment. Ground Water 30, 958–964.

McCarthy, J.F., Jimenez, B.D., 1985. Interactions between polycyclic aromatic hydrocarbons and dissolved humic material: binding and dissociation. Environ. Sci. Technol. 19, 1072–1076.

Molson, J.W., Frind, E.O., Van Stempvoort, D.R., Lesage, S., 2001. Humic acid enhanced remediation of an emplaced diesel source in groundwater: Part 2. Numerical model development and application. J. Contam. Hydrol. (this issue).

Neu, T.R., Swerhone, G.D.W., Lawrence, J.R., 2001. Assessment of lectin-binding-analysis for in situ detection of glycoconjugates in biofilm systems. Microbiology 147, 299–313.
Noordman, W.H., Bruining, J.-W., Wietzes, P., Janssen, D.B., 2000. Facilitated transport of a PAH mixture by a rhamnolipid biosurfactant in porous silica matrices. J. Contam. Hydrol. 44, 119–140.
Olson, J.J., Mills, G.L., Herbert, B.E., Morris, P.J., 1999. Biodegradation rates of separated diesel components. Environ. Toxicol. Chem. 18, 2448–2453.
Paulsen, J.E., Ekrann, S., Oppen, E., 1999. Visualisation of bacterial degradation and mobilisation of oil in a porous medium. Environ. Geol. 38, 204–208.
Rao, P.S., Annable, M.D., Sillan, R.K., Dai, D., Hatfield, K., Graham, W.D., Wood, A.L., Enfield, C.G., 1997. Field-scale evaluation of in situ cosolvent flushing for enhanced aquifer remediation. Water Resour. Res. 33, 2673–2686.
Ringelberg, D., Perkins, E., Hansen, L., Talley, J., Fredrickson, H., 1999. Relating biodegradation potentials to in-situ microbial community composition. In: Alleman, B.C., Leeson, A. (Eds.), In Situ Bioremediation of Petroleum Hydrocarbon and Other Organic Compounds, vol. 3. Battelle Press, Columbus, OH, pp. 545–550.
Roote, D.S., 1998. In Situ Flushing. Technology Status Report, TS-98-01, Ground-Water Remediation Technologies Analysis Centre, Pittsburg, PA, 41 p. (available as PDF file at website www.gwrtac.org).
Sabatini, D.A., Knox, R.C., Harwell, J.H., Wu, B., 2000. Integrated design of surfactant enhanced DNAPL remediation: efficient supersolubilization and gradient systems. J. Contam. Hydrol. 45, 99–121.
Shaw, D.G. (Ed.), 1989a. Hydrocarbons with Water and Seawater: Part I. Hydrocarbons C_5 to C_7. IUPAC Solubility Data Series, vol. 37. Pergamon, Oxford, pps. 59–192; 369–431.
Shaw, D.G. (Ed.), 1989b. Hydrocarbons with Water and Seawater: Part II. Hydrocarbons C_8 to C_{36}. IUPAC Solubility Data Series, vol. 38. Pergamon, Oxford, pp. 9–91.
Tebbe, C.C., Vahjen, W., 1993. Interference of humic acids and DNA extracted directly from soil in detection and transformation of recombinant DNA from bacteria and yeast. Appl. Environ. Microbiol. 59, 2657–2665.
Thomas, D.H., Delfino, J.J., 1991. A gas chromatographic/chemical indicator approach to assessing ground water contamination by petroleum products. Ground Water Monit. Rev., 90–100 (Fall issue).
Van Stempvoort, D.R., Lesage, S., 2002. Binding of methylated naphthalenes to concentrated aqueous humic acid. Adv. Environ. Res. (in press).
Van Stempvoort, D.R., Molson, J.W., Lesage, S., 2000. Sorption of Aldrich humic acid to a test aquifer material and implications for subsurface remediation. In: Ghabbour, E.A., Davies, G. (Eds.), Humic Substances: Versatile Components of Plants, Soils and Water. Royal Society of Chemistry, Cambridge, UK, pp. 153–163.
West, C.C., Harwell, J.H., 1992. Surfactants and subsurface remediation. Environ. Sci. Technol. 26, 2324–2330.
Whyte, L.G., Slagman, S.J., Pietrantonio, F., Koval, S.F., Lawrence, J.R., Inniss, W.E., Greer, C.W., 1999. Physiological adaptations involved in alkane assimilation at low temperatures by *Rhodococcus* sp. strain Q15. Appl. Environ. Microbiol 65, 2961–2968.
Xu, H., Lesage, S., Durham, L., 1994. The use of humic acids to enhance removal of aromatic hydrocarbons from contaminated aquifers. Part I: Laboratory studies. Proceedings, 4th Annual Symposium on Groundwater and Soil Remediation, September 21–23. Calgary, AB, Canada, pp. 635–645.

Environment Canada Environnement Canada

Canada

Canada Centre for Inland Waters
P.O. Box 5050
867 Lakeshore Road
Burlington, Ontario
L7R 4A6 Canada

National Hydrology Research Centre
11 Innovation Boulevard
Saskatoon, Saskatchewan
S7N 3H5 Canada

St. Lawrence Centre
105 McGill Street
Montreal, Quebec
H2Y 2E7 Canada

Place Vincent Massey
351 St. Joseph Boulevard
Gatineau, Quebec
K1A 0H3 Canada

Centre canadien des eaux intérieures
Case postale 5050
867, chemin Lakeshore
Burlington (Ontario)
L7R 4A6 Canada

Centre national de recherche en hydrologie
11, boul. Innovation
Saskatoon (Saskatchewan)
S7N 3H5 Canada

Centre Saint-Laurent
105, rue McGill
Montréal (Québec)
H2Y 2E7 Canada

Place Vincent-Massey
351 boul. St-Joseph
Gatineau (Québec)
K1A 0H3 Canada